Pol. J. Environ. Stud. Vol. XX, No. X (XXXX), 1-12
DOI: *10.15244/pjoes/221719* ONLINE PUBLICATION DATE: 2026-08-31

Original Research

Effect of Metal Complexation on Chlorination of Ciprofloxacin

Lei Fang[1, 2], Jinghan Ye[1, 2], Rongrong Jiang[1], Zhongjun Liang[3], Yongji Zeng[3], Miaomiao Ye[1]*

[1]College of Civil Engineering and Architecture, Zhejiang University, Hangzhou 310058, China
[2]Future Water Laboratory, Innovation Center of Yangtze River Delta, Zhejiang University, Jiaxing 314000, China
[3]Guangzhou Water Supply Company, Guangzhou 510600, China

Received: 18 March 2026
Accepted: 11 May 2026

Abstract

Ciprofloxacin can complex with metal ions by providing carboxyl, carbonyl, and piperazine groups containing N as ligands, thereby affecting its chemical reactions. In this paper, the complexation of ciprofloxacin with common metal ions, the effects of metal complexation and coexistence on chlorination, and the influencing factors have been investigated. The complexation products were characterized by UV absorption spectrum and FTIR, and it was speculated that ciprofloxacin was complexed with metal ions in a ratio of 2:1 in the form of a single dentate ligand or double dentate chelation. The chlorination degradation of ciprofloxacin followed pseudo-first-order reaction kinetics. The reaction rate constants increased by 20% and 160%, the formation of trihalomethane decreased by 11.7% and 36.1%, and the formation of haloacetic acids increased by 12.8% and 19.8% with the coexistence and complexation of Fe^{3+}, respectively, compared with the Fe^{3+} absence condition. In the complexation process, electron transport by metal changed the molecular structure and electron cloud density of ciprofloxacin and promoted the formation of strong oxidizing free radicals, resulting in a more obvious effect of ciprofloxacin by metal complexation than by coexistence during chlorination. With different metal complexation, the order of inhibition on trihalomethane formation was Ca^{2+}> Mn^{2+}> $Fe^{3+,}$ and the order of promotion on haloacetic acid formation was Mn^{2+} > Ca^{2+} > Fe^{3+}.

Keywords: ciprofloxacin, metal complexation, chlorination, disinfection by-products, influence factor

Introduction

Among synthetic organic compounds, antibiotic substances are frequently detected in surface water and groundwater due to their widespread application [1], with fluoroquinolone antibiotics exhibiting particularly high detection frequency [2]. As precursors to disinfection by-products (DBPs), the benzene rings, carboxyl groups, and carbon-carbon double bond in fluoroquinolone antibiotics serve as primary reaction sites for chlorination, yielding a series of compounds during chlorination disinfection [3, 4]. Zhang et al. [5] investigated the chlorination of enrofloxacin in drinking water distribution systems, identifying the formation of three trihalomethanes (THMs), three haloacetic acids (HAAs), and two nitrogenous disinfection by-products

*e-mail: yemiao008@zju.edu.cn
Tel.: +86-571-88206759
0000-0002-5546-1133

(N-DBPs). Through chlorination disinfection, antibiotics produce DBPs exhibiting cytotoxic, genotoxic, and mutagenic properties [6], thereby posing threats to human health. Consequently, the chlorination reaction process of antibiotics has attracted significant attention from researchers.

Meanwhile, metal ions are inorganic compounds widely present in aquatic environments. The discharge of industrial wastewater, the dissolution of metal compounds from riverbed sediments, and the use of metal coagulants in water treatment processes contribute to the increasing concentration of metal ions in surface water [7-10]. Antibiotic substances, rich in electron-donating groups [11], such as hydroxyl, carboxyl, and amino groups, interact with metal ions through adsorption, coagulation, and complexation. These interactions influence the migration and transformation patterns of antibiotic substances during water treatment processes. Therefore, the risk of combined pollution posed by antibiotics and metal ions during chlorination processes warrants attention.

Currently, several studies have reported the influence of metal ions on the chlorination reaction of organic compounds. Liu et al. [12] found that Fe^{3+} promoted the formation of total trihalomethanes and total haloacetic acids in raw water from the Yangtze River and Huangpu River. Zhang et al. [13] investigated the catalytic potential of copper corrosion products (Cu(II), Cu_2O, CuO) on chlorine decay and haloacetic acid formation. Their study demonstrated that the presence of soluble Cu(II) and surface-bound Cu(II) increases the extent of the reaction between natural organic matter (NOM) and chlorine. Zhao et al. [14] observed that adding 4 mmol Ca^{2+} to NOM (humic acid and fulvic acids) during chlorination increased the formation of trihalomethanes, dihaloacetic acids, and trihaloacetic acids by 24%~47%, 51%~61%, and 15%~25%, respectively. Previous research has primarily focused on the effects of coexisting metal ions on the formation of DBPs, while the influence of metal-organic interactions on chlorination reactions warrants further investigation.

Carboxyl groups form strong Ligand-to-Metal Charge-Transfer (LMCT) bands with metal ions in the near-ultraviolet and visible light regions [15]. Metal complexation not only reduces the overall pollutant levels but also affects the reaction activity of organic compounds [16, 17]. Studies indicate that fluoroquinolones can complex with various metal ions [18], forming relatively stable complexes, thereby influencing the adsorption, oxidative degradation, and photodegradation characteristics of antibiotics [19]. Zhang et al. [20] investigated norfloxacin degradation in algae-laden water, discovering that Fe^{3+} can form ligands with carboxylic acids, accelerating organic degradation. Similarly, in the photodegradation of tetracycline, both Fe^{2+} and Fe^{3+} promote degradation through complexation [21]. Batista et al. [22] evaluated the degradation effects of Fe^{3+} on two sulfonamide antibiotics under sunlight exposure, observing that the degradation efficiency of the two antibiotics increased by 20% and 19% within 70 minutes, respectively. Chen et al. [23] discovered that the complexation of Fe^{3+} with carboxyl groups promotes the degradation of penicillin antibiotics. Vione et al. [24] examined the photodegradation reactions of clarithromycin and roxithromycin, finding that complexation with Fe^{3+} accelerates the degradation of both antibiotics. The complexation of quinolone antibiotics with metal cations (Fe^{3+}, Al^{3+}, Zn^{2+}, Cu^{2+}, and Mg^{2+}) decreases antibacterial activity [25]. These studies collectively demonstrate that metal complexation significantly impacts the chemical reaction processes of organic pollutants.

Therefore, this study aims to investigate the influence of metal complexation on the degradation of antibiotic substances and the formation trend of disinfection by-products during chlorination. It focused on ciprofloxacin (CIP) as the target pollutant, and the selected metal ions included Fe^{3+}, Mn^{2+}, and Ca^{2+}. The complexation reactions between CIP and metal ions were examined, inferring the complex structure through characterization analysis. The impact mechanism of metal complexation versus metal coexistence on the chlorination of CIP was systematically investigated, including the reaction kinetics, degradation products, and DBPs. Furthermore, the influences of pH, metal ions, and coexisting organic matters on the chlorination of the Fe(III)-CIP complex were investigated. This study provided technical guidance for elucidating the interaction between metals and organic substances and its impact mechanism on water treatment processes.

Materials and Methods

Chemicals

Ciprofloxacin (≥99%), sodium hypochlorite (NaClO, 6%~14%), $Fe_2(SO_4)_3 \cdot xH_2O$, $MnSO_4 \cdot 4H_2O$, $CaSO_4 \cdot 2H_2O$, sodium thiosulfate, anhydrous sodium sulfate, sulfuric acid, and other chemical reagents were purchased from Sinopharm Chemical Reagent Company (Shanghai, China). Chromatographic-grade methanol, acetonitrile, and methyl tert-butyl ether (MTBE) were purchased from Aladdin Reagent Company (Shanghai, China). Four trihalomethane standard solutions (chloroform, bromodichloromethane, dibromochloromethane, and bromoform) and nine haloacetic acid standard samples (bromochloroacetic acid, bromodichloroacetic acid, chlorodibromoacetic acid, dibromoacetic acid, dichloroacetic acid, monobromoacetic acid, monochloroacetic acid, tribromoacetic acid, and trichloroacetic acid) were purchased from TMstandard (Beijing, China). N,N-Diethyl-1,4-phenylenediamine (DPD) chlorine reagent pack was obtained from HACH Company (Loveland, USA).

Experiment Procedure

Metal Complexation: 1 mg/L CIP solution was prepared and placed in a brown glass bottle. A solution of metal ions was added, and the mixture was placed in a constant-temperature shaker, with the reaction temperature set to 25ºC and the shaking speed set to 150 rpm for 6 h. Samples were taken at predetermined time intervals to investigate the effects of different complexation times and complexation ratios. After the complexation reaction, suspended particles were formed. Following filtration and drying, the complexes were prepared as powders.

Chlorination: Three sets of control experiments were conducted to investigate the differential effects of metal coexistence and complexation on the chlorination reaction of CIP by controlling the addition methods of metal ions. The experimental setups for the three sets are as follows: 1 mg/L CIP and 1 mg/L sodium hypochlorite were added as the control group; 1 mg/L CIP, 0.5 mg/L metal ions and 1 mg/L sodium hypochlorite were added simultaneously as the metal coexistence group; 1 mg/L CIP, 0.5 mg/L metal ions were complexed under the condition of (25ºC, pH = 7.0, 150 rpm) for 4 h, followed by the addition of sodium hypochlorite as the metal complexation group. In the three reaction sets, 0.1 mg/L Br^- was added to promote the formation of DBPs. At 24 h into the reaction, excess sodium thiosulfate solution was added to quench residual chlorine. Water samples were taken for CIP degradation trend analysis and DBPs analysis. Parallel groups were established for all experiments.

Analytical Methods

UV-visible spectrophotometer (UV-vis) (DR-6000, HACH, USA), Fourier Transform Infrared Spectrometer (FTIR) (Spectrum Two, PE, USA), and X-ray Photoelectron Spectroscopy (XPS) (ESCALAB 250Xi, TFS, USA) were employed for the characterization analysis of the complexes. Chlorine concentration was detected using the DPD spectrophotometry at a detection wavelength of 530 nm.

CIP was measured using an Agilent 1200 High-Performance Liquid Chromatography (HPLC) system (Agilent Technologies, USA) equipped with a UV detector. A Zorbax Eclipse XDB-C18 column (4.6 mm × 150 mm, 5 μm particle size) was used with a detection wavelength of 278 nm and a column temperature of 40ºC. The mobile phase consisted of acetonitrile/0.1% phosphoric acid (25/75, v/v) at a flow rate of 0.8 mL/min. CIP degradation products were analyzed using an Agilent 6460 High-Performance Liquid Chromatography-Triple Quadrupole Tandem Mass Spectrometry (HPLC-TQTMS) system (Agilent Technologies, USA) and QP 2010 Plus Gas Chromatography-Mass Spectrometer (GC-MS) (Shimadzu Corporation, Japan).

Trihalomethanes and haloacetic acids, two classes of halogenated disinfection byproducts, were analytically detected using Thermo Trace 1300 Gas Chromatograph-Electron Capture Detector (GC/ECD) (Thermo Fisher Scientific, USA). The chromatographic column employed was an HP-5 capillary column (30 m × 0.32 mm × 0.25 μm). Samples for THM analysis were pretreated with MTBE for liquid-liquid extraction. The instrument conditions were set to an injector temperature of 210ºC and a detector temperature of 290ºC. The temperature program was as follows: initial temperature was 35ºC, held for 13 min, then increased to 200ºC at 30ºC/min and held for 3 min. For HAAs, samples underwent liquid-liquid extraction with MTBE followed by derivatization reaction pretreatment with sulfuric acid-methanol solution. The instrument conditions were set to an injector temperature of 175ºC and a detector temperature of 300ºC. The gradient temperature program was as follows: initial temperature was 35ºC, holding for 5 min, increased to 90ºC at a rate of 5ºC/min, and held for 5 min.

Results and Discussion

Metal Complexation Reactions

This study investigated the effects of complexation reaction parameters on UV absorption spectra of metal-CIP complexes, including complexation time, complexation ratio, and metal type, and the results are shown in Fig. 1. As observed, the UV absorption spectrum of the metal-CIP complex exhibits significant changes, with a pronounced decrease at 278 nm. The complexation time had a negligible effect on the complexation between CIP and Fe^{3+}. CIP and the metal ion likely form a relatively stable complex via strongly covalent functional groups, without exhibiting re-hydrolysis over time.

As shown in Fig. 1b), the absorption spectra of CIP exhibited varying degrees of deviation upon complexation with different ratios of iron ions. The comparison between calculated and measured UV absorption spectra revealed significant peak shifts for the Fe(III)-CIP complexes across the 0.6:1 to 4:1 ratio range, with the most pronounced difference occurring at a 2:1 ratio. Lopez et al. [26] discovered that CIP forms three complexes with copper at 1:1 or 1:2 ratios. Ouyang et al. [27] compared the complexation of Fe^{3+} with three carboxylic acids (CA, TA, MA) and found that they achieve optimal complexation states with Fe^{3+} at different ratios. Antibiotics form distinct complexes with different metal ions at varying complexation ratios. Fig. 1c) compares the complexation of CIP with Fe^{3+}, Mn^{2+}, and Ca^{2+}, showing the most pronounced UV absorption spectrum changes for Fe^{3+}, followed by Mn^{2+}, and Ca^{2+} exhibiting the least variation. Brillault et al. [28] determined the complexation constants of CIP with five metal ions, which followed the order: $Cu^{2+} > Al^{3+} > Zn^{2+} > Mg^{2+} > Ca^{2+}$, which generally aligns with the order of electron-withdrawing ability of these metal ions.

The complexation ability of the metal ion is influenced by both the electron-withdrawing capacity and the steric hindrance effect. Therefore, the order of complexation capacities in this study is likely Fe^{3+} >Mn^{2+} >Ca^{2+}. Subsequent experiments will primarily focus on the complexation of CIP with Fe^{3+}.

FTIR and X-ray photoelectron spectroscopy were employed in this study to characterize the Fe(III)-CIP complex, with the aim of elucidating its structure. The corresponding results are presented in Fig. 2(a-e). The infrared spectral characterization of CIP revealed a characteristic peak at 1707 cm^{-1} corresponding to the C=O stretching vibration of the carboxyl group, which disappeared upon complexation. The peak at 1272 cm^{-1} represents the cooperative action of C-O stretching and O-H bending vibrations of the carboxyl group, with diminished intensity observed in the Fe(III)-CIP complex. Additionally, a new peak corresponding to the COO-Fe stretching vibration appeared at approximately 1144 cm^{-1}. These spectral band variations indicate that the complexation between CIP and Fe^{3+} induced vibrational shifts in the functional groups. XPS analysis revealed that the C 1s, O 1s, and Fe 2p binding energies shifted to lower values in the Fe(III)-CIP complex compared to the free CIP. The C 1s peaks of the free CIP were observed at 288.2, 285.8, and 284.6 eV, shifting to 288.1, 285.2, and 284.2 eV upon complexation. The two O 1s peaks of the free CIP correspond to O-H and O-R bonds, located at 532.1 eV and 530.7 eV, respectively. Upon complexation, these peaks correspond to O-H and O-Fe bonds and shift to 531.0 eV and 529.7 eV, respectively.

Gu et al. [29] investigated the adsorption of CIP on hydrous iron oxides, hypothesizing that CIP forms a complex through coordination of its carboxylate oxygen atoms to iron ions. Rakshit et al. [30] investigated the adsorption of CIP on nanomagnetite, discovering that CIP forms a bidentate binuclear complex through chelation of its two carboxylate oxygen atoms to two iron ions. Therefore, in this study, the coordination between CIP and metal ions may occur either via a monodentate complex involving the carbonyl oxygen

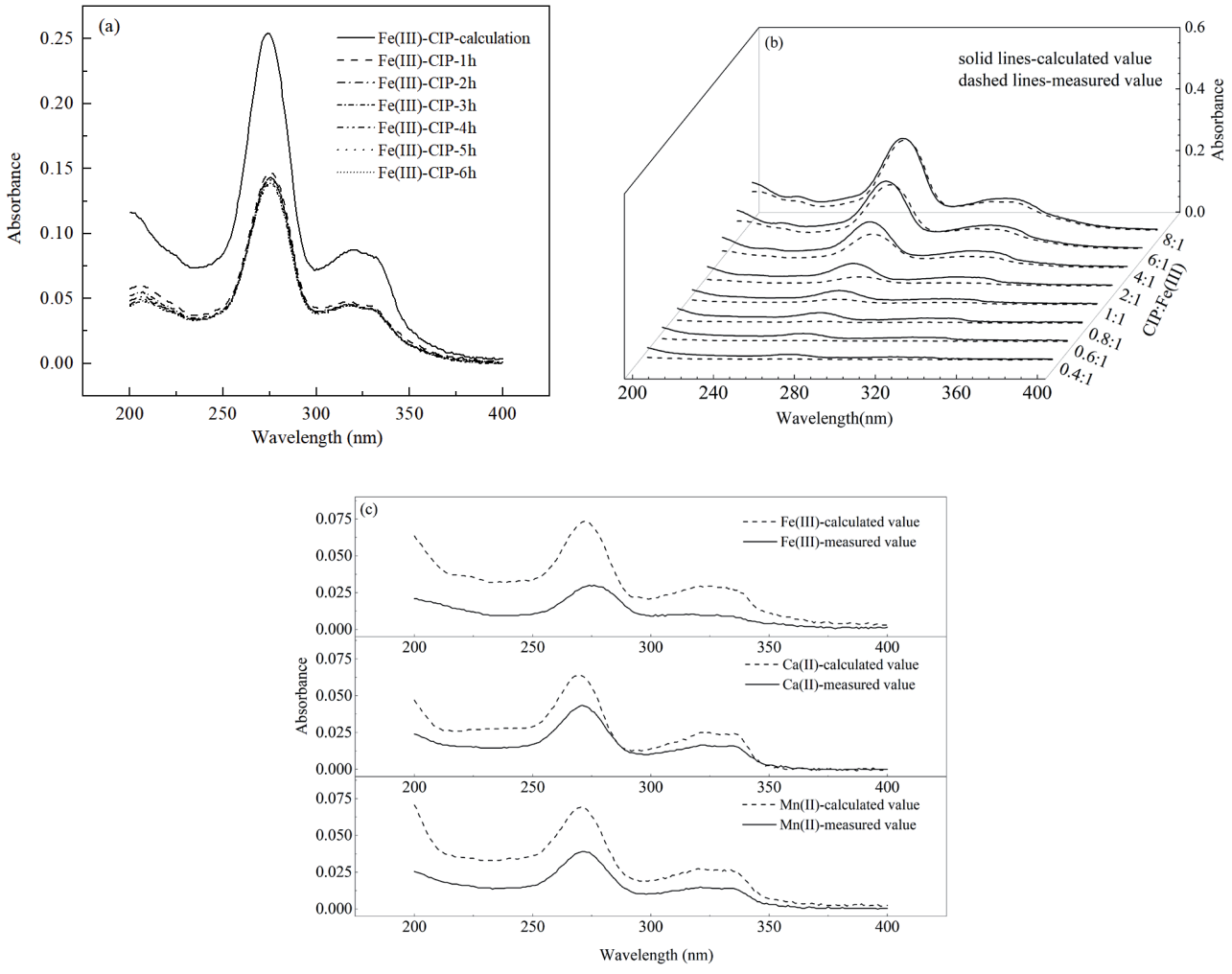

Fig. 1. Ultraviolet absorption spectrum of the complexes between CIP and metal ions: a) Complexation time (Fe^{3+}); b) Complexation ratio (Fe^{3+}); c) Metal ions.

or via a bidentate chelate involving both oxygen atoms of the carboxyl group. The change in XPS binding energy indicates electron transfer occurs during the complexation of CIP with Fe^{3+}. DFT calculations show charge redistribution upon complexation, and the charges shift from O_1 (-0.294) and O_2 (-0.448) to O_1 (-0.039) and O_2 (0.162), respectively, indicating electron transfer between oxygen and iron that alters the electron density distribution of CIP. Combined with the characterization analysis, the proposed structure of the Fe(III)-CIP complex is depicted in Fig. 2f).

Chlorination of Ciprofloxacin

Degradation Kinetics

The addition of metal ions during chlorination alters the degradation of organic compounds and the formation of DBPs [31]. Fig. 3a) presents the chlorination degradation kinetics of CIP under three different conditions: Fe^{3+} complexation, Fe^{3+} coexistence, and Fe^{3+} absence. The results indicate that CIP degradation follows pseudo-first-order reaction kinetics, with rate constants of 0.26 h^{-1}, 0.12 h^{-1}, and 0.10 h^{-1} under Fe^{3+} complexation, Fe^{3+} coexistence, and Fe^{3+} absence conditions, respectively. Both Fe^{3+} complexation and Fe^{3+} coexistence promote the chlorination degradation of CIP to some extent. Yao et al. [32] observed that the addition of iron ions increased the degradation rate constant of tetracycline by 50% in their study of tetracycline photodegradation. Cai et al. [33] found that the complexation of Cu(II) enhanced the degradation of tetracycline in the ferrous sulfide/sulfite system, raising the degradation rate from 15.6% to 76.1%. In this experiment, the degradation rate constant of CIP increased by 160% and 20% under Fe^{3+} complexation and Fe^{3+} coexistence conditions, respectively. Complexed Fe^{3+} promoted the chlorination degradation of CIP to a greater extent than free Fe^{3+}. Through intramolecular electron transfer, the formed metal-antibiotic complexes alter the antibiotic structure and electron density, while generating free radicals. Acting as electron carriers, metal ions promote the oxidative degradation of antibiotics.

Formation of THMs and HAAs

Chlorination of CIP typically generates C-DBPs. This study analyzed and compared the formation of DBPs during CIP chlorination under three conditions: Fe^{3+} complexation, Fe^{3+} coexistence, and Fe^{3+} absence, as shown in Fig. 3b) and c). Under all three conditions, DBP formation increased rapidly within 8 h and then gradually increased from 8 to 48 h. Compared to the absence of Fe^{3+}, THM formation was suppressed, decreasing by 35.9% and 11.6% at 48 hours under Fe^{3+} complexation and Fe^{3+} coexistence, respectively. Conversely, HAA formation increased by 34.2% and 20.0%, respectively, with no significant differences observed among the groups. These different trends are explained by the distinct formation mechanisms of the DBPs.

The formation of THMs involves a multi-step reaction, where precursors first react with chlorine to form intermediates, which subsequently undergo hydrolysis, decarboxylation, or ring-opening to generate THMs. LIU et al. [34] proposed that altered electron density may influence the electrophilic substitution reaction activity between chlorine and the corresponding carbon atom, thereby reducing THM production. During the complexation between CIP and metal ions, both the electron density and the vibration of the carboxyl or carbonyl group on CIP are altered, thereby affecting THM formation. The formation of HAAs is related to the structure and molecular weight of DBP precursors and is significantly proportional to hydroxyl radical concentration [21]. Increased hydroxyl radicals promote aromatic ring cleavage, positively influencing the formation of small molecules and the conversion of intermediates into HAAs [34]. The presence of metal ions alters the structure of CIP, catalyzing the generation of more hydroxyl radicals, which in turn affects HAA formation.

Degradation Mechanism

During the chlorination of CIP involving metal complexation, LC-MS analysis of the reaction products revealed that the intermediate compounds formed primarily resulted from substitution, ring-opening, and hydroxylation reactions. The proposed degradation pathway of CIP is illustrated in Fig. 4, primarily comprising: (1) Substitution of chlorine at the C(1) position of the quinolone ring to form P1, followed by chlorine-mediated cleavage of the piperazine ring to yield R2, which finally undergoes hydroxylation at the amino group to form product P3; (2) Chlorine replaces hydrogen on the piperazine nitrogen to form intermediate R1, followed by chlorine-mediated cleavage of the piperazine ring to yield product P2. As the reaction proceeds, the piperazine ring is completely cleaved to form R3. The amino group is either chlorinated by hypochlorous acid to produce R4 or substituted by hydroxyl radicals to form R5.

To further elucidate the degradation mechanism of CIP, DFT calculations were performed at the B3LYP/6-311++G (d,p) level using Gaussian 09 to obtain the total charge distribution and HOMO value of the ciprofloxacin molecule; the computational results are shown in Fig. 5. The figure indicates that the negative charges on atoms in CIP are relatively high at C(1), C(8), O(14), and O(15), making these atoms prone to electron loss, thereby forming radical intermediates. Following complexation, CIP exhibits higher negative charges at C(1), C(5), C(6), N(17), and N(20), presenting more sites susceptible to chlorination, thereby enhancing the chlorination rate. Prior to complexation, the preferred reaction sites during chlorination likely occur at C(3),

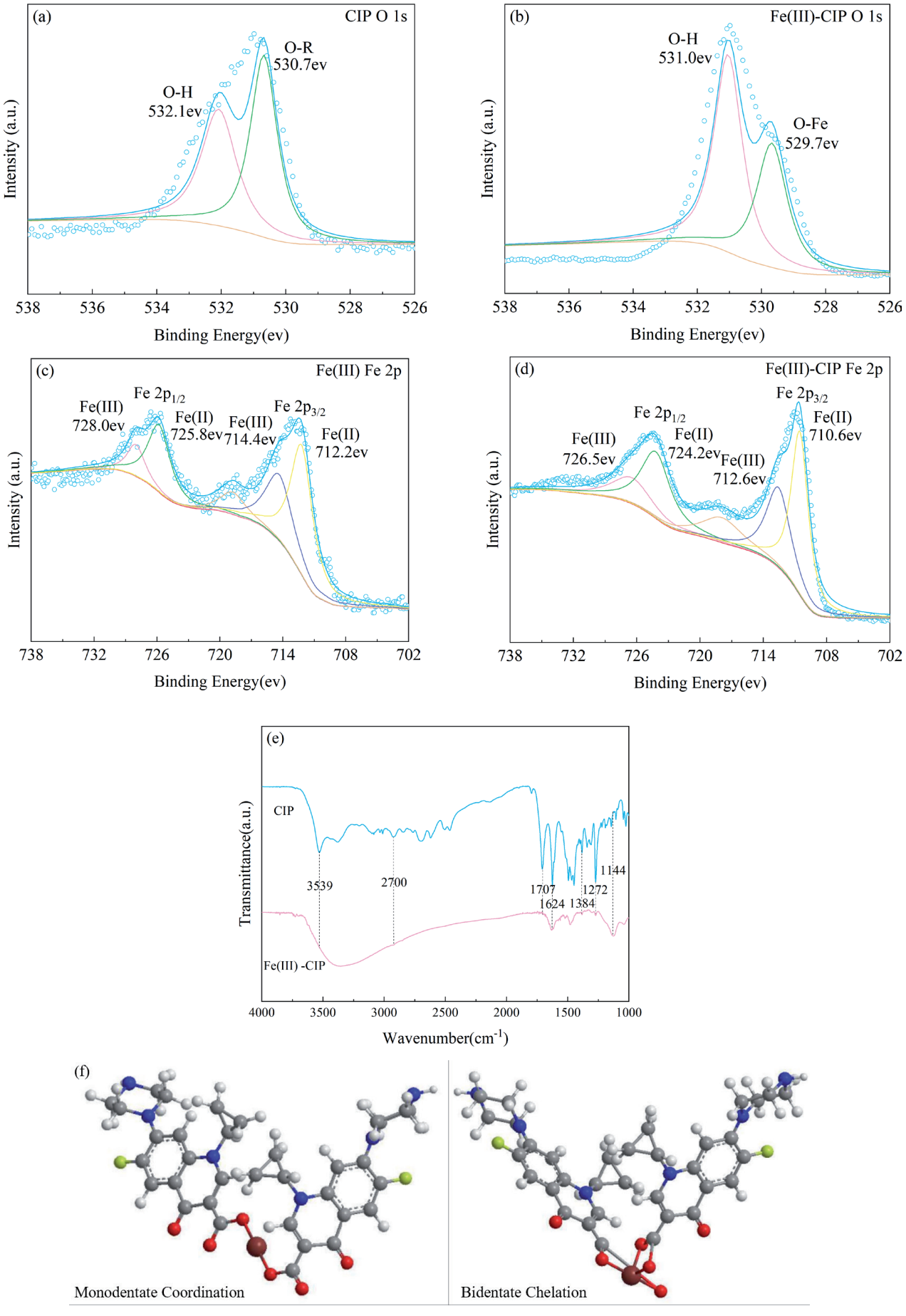

Fig. 2. a-d) XPS of the Fe(III)-CIP complex; e) FTIR of the Fe(III)-CIP complex; f) Potential complexation sites for metal ions in CIP.

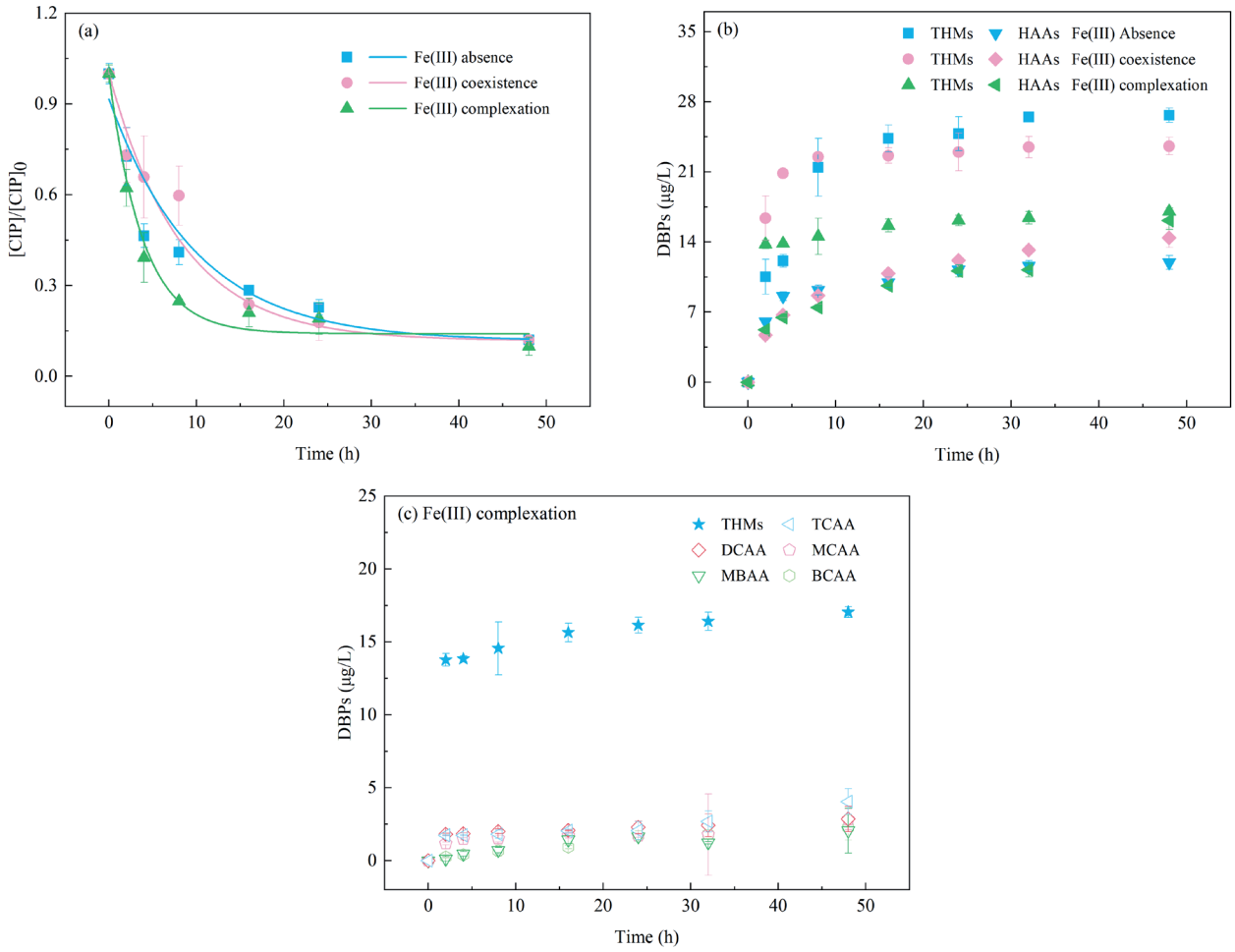

Fig. 3. Degradation and DBP formation from CIP: a) Degradation kinetics; b) Comparison of DBP formation under three systems; c) Chlorination of CIP after complexation with Fe^{3+} to form DBPs.

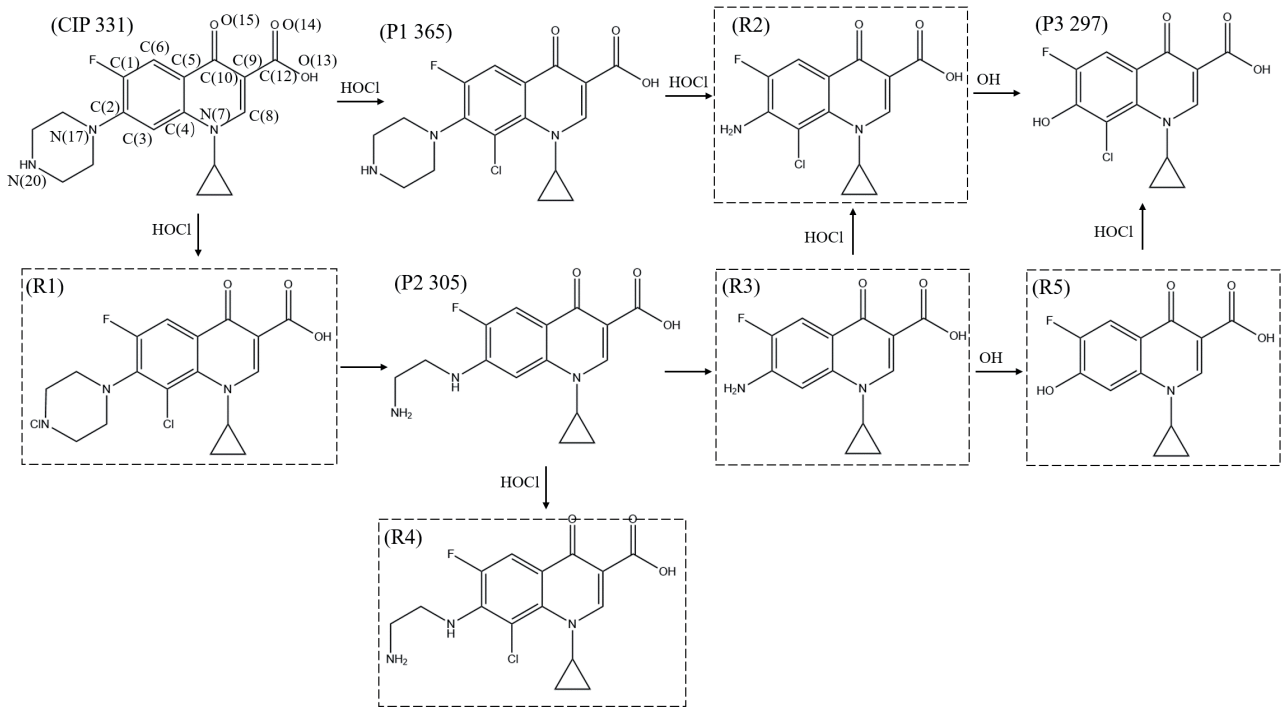

Fig. 4. Analysis of the chloride degradation product pathway of the Fe(III)-CIP complex.

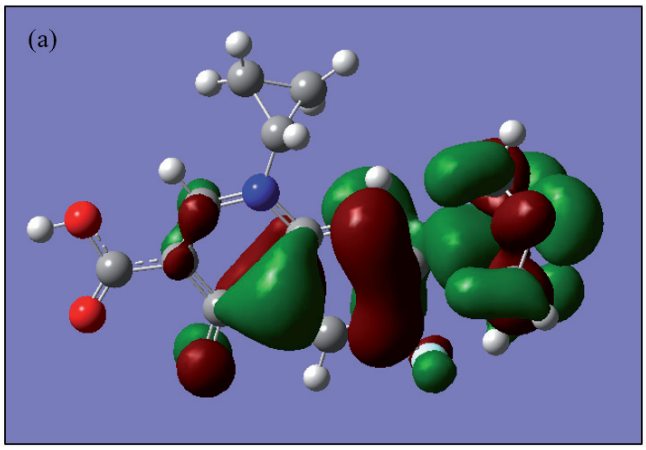

(b)

NO.	Atom	charge		$2FED^2_{HOMO}$		NO.	Atom	charge		$2FED^2_{HOMO}$	
		Before	After	Before	After			Before	After	Before	After
1	C	–0.839	–9.034	0.127	0.198	13	O	–0.294	–0.039	0.001	0.004
2	C	0.203	11.534	0.131	0.129	14	O	–0.448	0.162	0.003	0.004
3	C	–0.296	0.023	0.166	0.043	15	O	–0.514	–0.565	0.056	0.084
4	C	–0.049	–0.146	0.047	0.165	16	C	–0.388	–0.155	0.001	0.007
5	C	0.781	–4.148	0.177	0.110	17	N	0.102	–0.281	0.564	0.053
6	C	0.008	–6.519	0.035	0.396	18	C	–0.215	–3.221	0.081	0.027
7	N	0.427	0.723	0.005	0.057	19	C	–0.331	2.165	0.074	0.020
8	C	–0.884	–0.103	0.017	0.088	20	N	–0.363	–0.408	0.132	0.007
9	C	0.872	0.881	0.013	0.046	21	C	–0.217	–0.175	0.071	0.008
10	C	–0.548	–0.560	0.035	0.084	22	C	–0.275	0.254	0.077	0.009
11	F	–0.187	9.000	0.028	0.184	23	C	–0.174	–0.470	0.001	0.002
12	C	0.504	–0.695	0.002	0.015	24	C	–0.461	–0.423	0.000	0.002

Fig. 5. DFT calculations for the CIP chlorination process: a) HOMO orbital of CIP; b) Frontier electron density of atoms in CIP before and after complexation.

C(5), and N(17) with higher $2FED^2_{HOMO}$ values. After complexation, C(1), C(2), C(4), and C(6) exhibit higher $2FED^2_{HOMO}$ values, making them more likely to undergo electrophilic reactions with chlorine. The metal binds to the oxygen atoms in the CIP carboxyl group via either monodentate or bidentate coordination, thereby enhancing chlorine oxidation by altering the charge distribution across the atoms in CIP. Additionally, complexation modifies the HOMO values of individual atoms, altering the electrophilic reaction sites, thereby influencing the preferred reaction sites for chlorine. This leads to a greater diversity and yield of products than those formed during chlorination of free CIP alone.

Influencing Factors

Metal Ions

A comparative study was conducted on the effects of complexation with three different metal ions on the chlorination reaction of CIP. Fig. 6a) shows the degradation of CIP at 24 hours. Compared to the absence of metal ions, CIP degradation was enhanced by 18.1%~19.6% via complexation and by 3.7%~15.6% via coexistence. The promoting effect of the metal complexes on CIP degradation followed the order: Ca^{2+}>Fe^{3+}>Mn^{2+}. As shown in Fig. 6b) and c), metal ions suppressed THM formation while promoting HAA generation. Compared to the metal-free control, metal complexation reduced THM production by 13.8%~58.9% and increased HAA generation by 22.5%~50.7%, whereas the coexistence of metal ions reduced THM production by 7.6%~36.7% and increased HAA generation by 2.8%~22.5%. Metal ions exerted a significantly stronger effect in the complexed state than in the coexisting state. Overall, metal complexation reduced THMs by 0.2 μg/L~5.0 μg/L and increased HAAs by 0.4 μg/L~2.5 μg/L, relative to metal coexistence. Specifically, for THM formation, complexation had little effect for Fe^{3+} and Mn^{2+} compared to coexistence, but markedly enhanced inhibition for Ca^{2+}. For HAAs, while Mn^{2+} showed negligible difference between the two conditions, complexation of Fe^{3+} and Ca^{2+} significantly promoted HAA formation relative to coexistence.

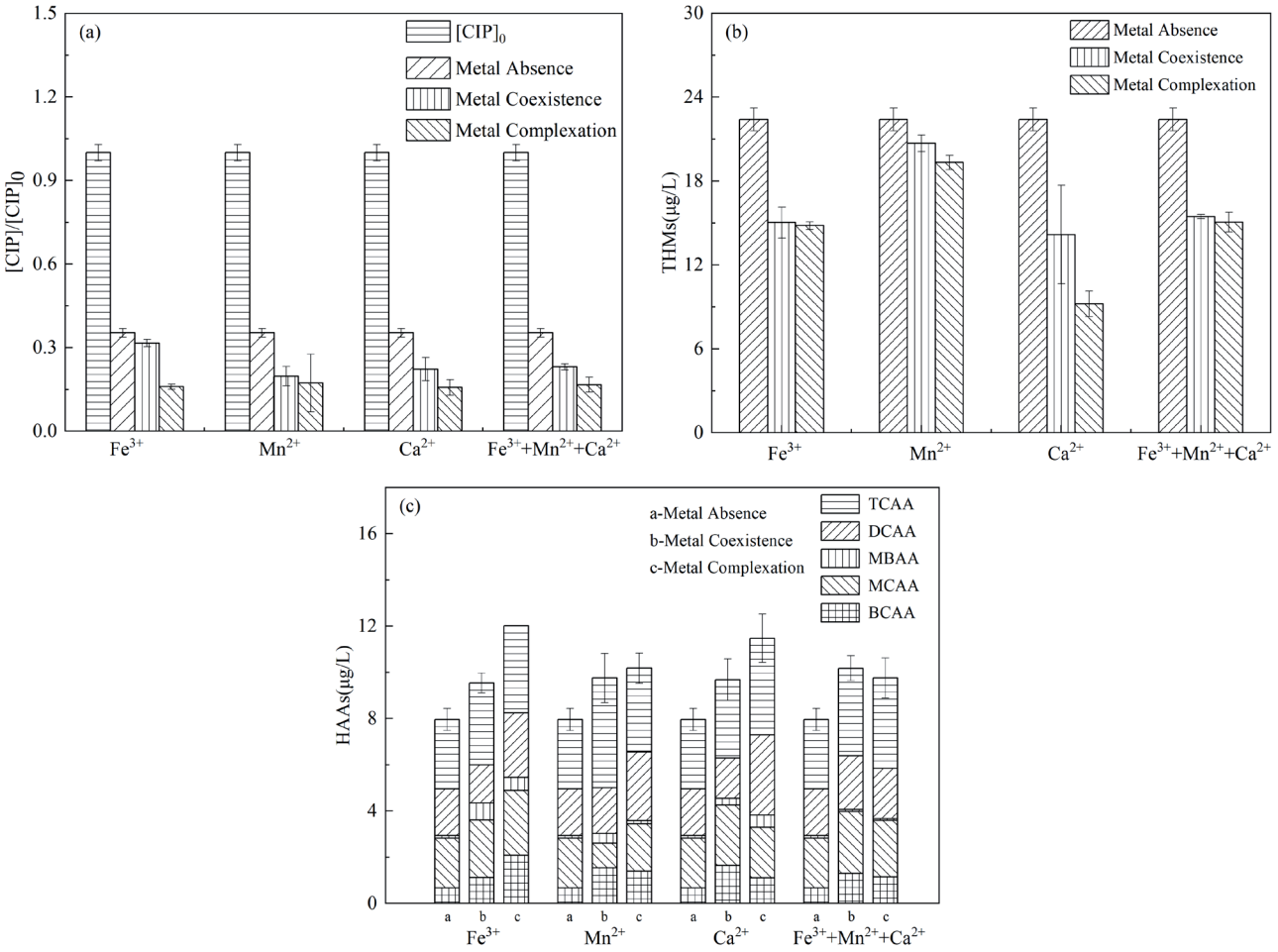

Fig. 6. Effects of different metal ions on the chlorination degradation of CIP: a) CIP; b) THMs; c) HAAs.

In this study, the inhibitory order of metal complexation on THM formation was Ca^{2+}>Fe^{3+}>Mn^{2+}; the promoting order on HAA formation was Fe^{3+}>Ca^{2+}>Mn^{2+}. The mechanism of action, whether through coexistence or complexation, was qualitatively consistent across all three metal ions and with that of individual ions: each promoted CIP degradation and enhanced HAA formation while suppressing THM generation. However, no regular synergistic effects were identified. This is likely attributed to competition among metal ions preventing stable formation of metal-CIP complexes, thereby disrupting subsequent chlorination reactions. Consequently, mixed metal ions exhibit a less pronounced effect than that induced by complexation with individual ions.

pH

CIP possesses two acid dissociation constants corresponding to its two chemical groups: the carboxyl group and the piperazine group [35]. As pH varies, CIP exists in three states: cationic (CIP^+), zwitterionic (CIP^0), and anionic (CIP^-) [36]. This pH-dependent speciation affects its complexation and chlorination reactions. As shown in Fig. 7a), the 24-hour chlorination degradation efficiencies of CIP were 61.3%, 74.6%, and 95.5% at pH 5, 7, and 9, respectively, indicating a clear positive correlation with pH. In studying the effect of iron ions on enrofloxacin photodegradation, Sciscenko et al. [37] observed that the degradation rate constant at pH 7 increased by an order of magnitude compared to pH 3. This can be attributed to more active metal-antibiotic complexation under neutral and alkaline conditions, which promotes the generation of free radicals, thereby accelerating antibiotic degradation.

Under alkaline conditions, Fe^{3+} exhibits a greater propensity to promote the formation of DBPs during CIP chlorination. As shown in Fig. 7a), compared to acidic conditions (pH 5), chlorination of CIP following complexation with Fe^{3+} under neutral and alkaline conditions (pH 9) resulted in increases of 2.9 μg/L and 15.5 μg/L in THM formation, and 1.3 μg/L and 1.8 μg/L in HAA formation, respectively. Under low pH conditions, CIP is protonated to form CIP^+. This occurs via the addition of a proton to the secondary amine nitrogen of the piperazine ring, generating a positively charged ammonium group (NH_2^+). As the pH increases, the CIP^+ undergoes initial deprotonation at the carboxyl group to form CIP^0. In this state, the negatively charged carboxylate (COO^-) balances the positively charged

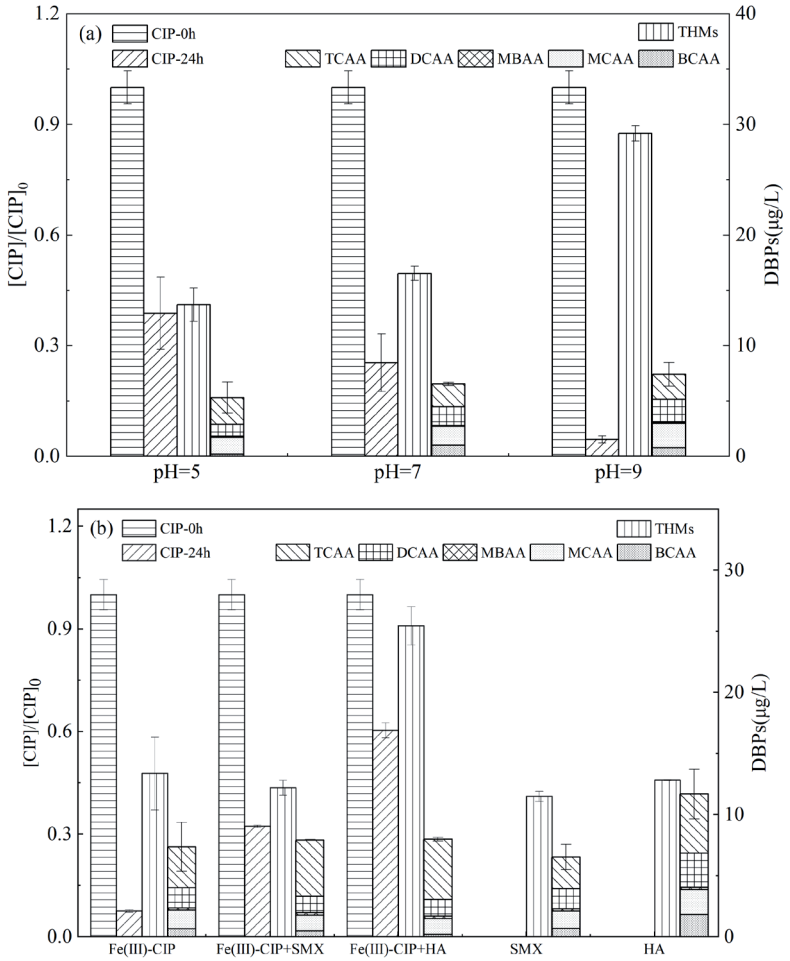

Fig. 7. Effect of pH and Coexisting organic matter on the chlorination reaction of Fe(III)-CIP complex: a) pH; b) Coexisting organic matter.

piperazine ammonium group (NH_2^+), resulting in a net neutral species. Upon a further increase in pH, the CIP^0 loses a second proton from the piperazine ammonium group, converting it back to a neutral amine (NH) and thereby yielding CIP^-. The three states of CIP at different pH levels alter its complexation reactions with metal ions, affecting the formation of chlorinated products. Specifically, alkaline conditions favor the increased generation of hydroxyl radicals, promoting the hydrolysis of chlorinated intermediates.

Coexisting Organic Compounds

Organic compounds compete with CIP for complexation with Fe^{3+} and its chlorination reaction. Sulfamethoxazole (SMX) and humic acid (HA) were selected as representative compounds to compare their respective influences on DBP generation from chlorination of the Fe(III)-CIP complex. Fig. 7b) shows that the presence of organic compounds significantly impedes the chlorination degradation of CIP. In the three systems, the degradation efficiencies of CIP at 24 h were 92.5%, 67.7%, and 39.6%, respectively. Both SMX and HA inhibited CIP degradation by competing for oxidants, but HA exhibited a significantly stronger inhibitory effect than SMX.

When chlorinated individually, the Fe(III)-CIP complex, SMX, and HA generated THMs at 13.4, 11.5, and 12.8 μg/L, and HAAs at 7.4, 7.9, and 8.0 μg/L, respectively. Due to competition among organic compounds for metal ions and chlorine, which influences DBP formation, when SMX coexists with the Fe(III)-CIP complex, the DBP yield decreased compared to that from the complex alone; when HA coexists with the complex, the yield increased yet remained below the sum of the yields from HA and the Fe(III)-CIP complex chlorinated separately. Wang et al. [38] found that the chlorination of CIP produced fewer DBPs in the presence of other organic compounds than when chlorinated alone. Furthermore, π-π stacking between the benzene rings of CIP and coexisting organic compounds can occur, which modulates the CIP chlorination reaction through hydrogen bonding and hydrophobic interactions, thereby inhibiting DBP formation.

Conclusions

This study systematically investigated the chlorination of ciprofloxacin under metal complexation, with a focus on the reaction kinetics, the formation trends of DBPs, and the influencing factors. Characterization of the Fe(III)-CIP complex suggested that CIP binds to the metal ions at the carboxylate oxygen atoms via either monodentate complexation or bidentate chelation. The study revealed that metal ions enhanced the chlorination rate constants of CIP by 20% and 160% in the coexistence and complexation states, respectively, which is attributed to their role as electron carriers that markedly accelerate the chlorination degradation process. The complexation of CIP with metal ions enhances the generation of strongly oxidizing radicals and alters the group reactivity and electron density of CIP, resulting in a more pronounced effect of metal ions on the chlorination reaction in the complexed state compared to the coexisting state. DFT calculations indicate that complexation additionally alters the HOMO values of individual atoms, shifting the electrophilic reaction sites and thereby influencing the preferred reaction sites for chlorination, which successfully explains the experimentally observed increase in both the diversity and yield of chlorinated products relative to the chlorination of CIP alone. During chlorination, the impact of metal complexation on DBP formation is ion-specific: it suppresses THM formation in the order: Ca^{2+}>Fe^{3+}>Mn^{2+}, while promoting HAA formation in the order: Fe^{3+} >Ca^{2+} >Mn^{2+}. Furthermore, pH influences hydroxyl radical generation, with alkaline conditions potentially favoring hydroxyl radical formation and thereby promoting the production of DBPs.

Acknowledgments

This research was supported by the Zhejiang Provincial Natural Science Foundation of China (No. LY24E080005) and the National Key Research and Development Program of China (No. 2023YFF0614500, No. 2023YFC3208200).

Conflict of Interest

The authors declare no conflict of interest.

References

1. LI Z., LI M., ZHANG Z., LI P., ZANG Y., LIU X. Antibiotics in aquatic environments of China: A review and meta-analysis. Ecotoxicology and Environmental Safety, **199**, 110668, **2020**.
2. ORIMOLADE B., OLADIPO A., IDRIS A., USISIPHO F., AZIZI S., MAAZA M., LEBELO S., MAMBA B. Advancements in electrochemical technologies for the removal of fluoroquinolone antibiotics in wastewater: A review. Science of the Total Environment, **881**, 163522, **2023**.
3. NETH N., CARLIN C., KEEN O. Emerging investigator series: transformation of common antibiotics during water disinfection with chlorine and formation of antibacterially active products. Environmental Science: Water Research & Technology, **5** (7), 1222, **2019**.
4. WANG X., LI Y., LI R., YANG H., ZHOU B., WANG X., XIE Y. Comparison of chlorination behaviors between norfloxacin and ofloxacin: Reaction kinetics, oxidation products and reaction pathways. Chemosphere, **215**, 124, **2019**.
5. ZHANG T., HE G., DONG F., ZHANG Q., HUANG Y. Chlorination of enoxacin (ENO) in the drinking water distribution system: Degradation, byproducts, and toxicity. Science of the Total Environment, **676**, 31, **2019**.
6. DU Y., WU Q., LU Y., HU H., YANG Y., LIU R., LIU F. Increase of cytotoxicity during wastewater chlorination: Impact factors and surrogates. Journal of Hazardous Materials, **324**, 681, **2017**.
7. MOKARRAM M., SABER A., SHEYKHI V. Effects of heavy metal contamination on river water quality due to the release of industrial effluents. Journal of Cleaner Production, **277**, 123380, **2020**.
8. LI Y., WANG Z., CAI Y., XIAO K., GUO Z., PAN F. High resolution dissolved heavy metals in sediment porewater of a small estuary: Distribution, mobilization and migration. Science of the Total Environment, **905**, 167238, **2023**.
9. ARAB K., THOMPSON D., OLIVER I. Evaluation and characterisation of metal sorption and retention by drinking water treatment residuals (WTRs) for environmental remediation. International Journal of Environmental Science and Technology, **19** (8), 7727, **2022**.
10. WANG L., AL-DHABI N.A., HUANG X., LUAN Z., TANG W., XU Z., XU W. Suitability of inorganic coagulants for algae-laden water treatment: Trade-off between algae removal and cell viability, aggregate properties and coagulant residue. Journal of Hazardous Materials, **471**, 134314, **2024**.
11. WANG Q., HE X., XIONG H., CHEN Y., HUANG L. Structure, mechanism, and toxicity in antibiotics metal complexation: Recent advances and perspectives. Science of the Total Environment, **848**, 157778, **2022**.
12. LIU S., ZHU Z., QIU Y., ZHAO J. Effect of ferric and bromide ions on the formation and speciation of disinfection byproducts during chlorination. Journal of Environmental Sciences, **23** (5), 765, **2011**.
13. ZHANG H., ANDREWS S. Catalysis of copper corrosion products on chlorine decay and HAA formation in simulated distribution systems. Water Research, **46** (8), 2665, **2012**.
14. ZHAO Y., YANG H., LIU S., TANG S., WANG X., XIE Y. Effects of metal ions on disinfection byproduct formation during chlorination of natural organic matter and surrogates. Chemosphere, **144**, 1074, **2016**.
15. LI J., WU F., MAILHOT G., DENG N. Photodegradation of chloroform in aqueous solution: Impact of montmorillonite KSF particles. Journal of Hazardous Materials, **174** (1-3), 368, **2010**.
16. HU Q., LOU M., WANG R., BAI S., GUO H., ZHOU J., MA Q., WANG T., ZHU L., ZHANG X. Complexation with Metal Ions Affects Chlorination Reactivity of Dissolved Organic Matter: Structural Reactomics of Emerging Disinfection Byproducts. Environmental Science & Technology, **58** (31), 13890, **2024**.

17. POOLE K. At the Nexus of Antibiotics and Metals: The Impact of Cu and Zn on Antibiotic Activity and Resistance. Trends in Microbiology, **25** (10), 820, **2017**.
18. TUREL I. The interactions of metal ions with quinolone antibacterial agents. Coordination Chemistry Reviews, **232** (1-2), 27, **2002**.
19. CHEN Z., HE G., YOU T., ZHANG T., LIU B., WANG Y. Complex pollution of Fluoroquinolone antibiotics and metal oxides/metal ions in water: a review on occurrence, formation mechanisms, removal and ecotoxicity. Journal of Environmental Chemical Engineering, **12** (2), 112191, **2024**.
20. ZHANG J., FU D., WU J. Photodegradation of Norfloxacin in aqueous solution containing algae. Journal of Environmental Sciences, **24** (4), 743, **2012**.
21. WANG H., YAO H., SUN P., LI D., HUANG C. Transformation of Tetracycline Antibiotics and Fe(II) and Fe(III) Species Induced by Their Complexation. Environmental Science & Technology, **50** (1), 145, **2016**.
22. BATISTA A., COTTRELL B., NOGUEIRA R. Photochemical transformation of antibiotics by excitation of Fe(III)-complexes in aqueous medium. Journal of Photochemistry and Photobiology A: Chemistry, **274**, 50, **2014**.
23. CHEN J., WANG Y., QIAN Y., HUANG T. Fe(III)-promoted transformation of β-lactam antibiotics: Hydrolysis vs oxidation. Journal of Hazardous Materials, **335**, 117, **2017**.
24. VIONE D., FEITOSA-FELIZZOLA J., MINERO C., CHIRON S. Phototransformation of selected human-used macrolides in surface water: Kinetics, model predictions and degradation pathways. Water Research, **43** (7), 1959, **2009**.
25. SEEDHER N., AGARWAL P. Effect of metal ions on some pharmacologically relevant interactions involving fluoroquinolone antibiotics. Drug Metabolism and Drug Interactions, **25** (1-4), 17, **2010**.
26. LÓPEZ-GRESA M., ORTIZ R., PERELLÓ L., LATORRE J., LIU-GONZÁLEZ M., GARCÍA-GRANDA S., PÉREZ-PRIEDE M., CANTÓN E. Interactions of metal ions with two quinolone antimicrobial agents (cinoxacin and ciprofloxacin) - Spectroscopic and X-ray structural characterization. Antibacterial studies. Journal of Inorganic Biochemistry, **92** (1), 65, **2002**.
27. OUYANG Z., YANG C., HE J., YAO Q., ZHANG B., WANG H., JIANG Y., ZHOU J., DENG Y., LIU Y., YANG J., LU G., DANG Z. Homogeneous photocatalytic degradation of sulfamethazine induced by Fe (III)-carboxylate complexes: Kinetics, mechanism and products. Chemical Engineering Journal, **402**, 126122, **2020**.
28. BRILLAULT J., TEWES F., COUET W., OLIVIER J. In vitro biopharmaceutical evaluation of ciprofloxacin/metal cation complexes for pulmonary administration. European Journal of Pharmaceutical Sciences, **97**, 92, **2017**.
29. GU C., KARTHIKEYAN K. Sorption of the antimicrobial ciprofloxacin to aluminum and iron hydrous oxides. Environmental Science & Technology, **39** (23), 9166, **2005**.
30. RAKSHITA S., SARKAR D., ELZINGA E., PUNAMIYA P., DATTA R. Mechanisms of ciprofloxacin removal by nano-sized magnetite. Journal of Hazardous Materials, **246**, 221, **2013**.
31. QI W., LONG J., FENG C., FENG Y., CHENG D., LIU Y., XUE J., LI Z. Fe^{3+} enhanced degradation of oxytetracycline in water by pseudomonas. Water Research, **160**, 361, **2019**.
32. YAO H., PEI J., WANG H., FU J. Effect of Fe(II/III) on tetracycline degradation under UV/VUV irradiation. Chemical Engineering Journal, **308**, 193, **2017**.
33. CAI Y., SHEN S., FAN J. Enhanced degradation of tetracycline by Cu(II) complexation in the FeS/sulfite system. Journal of Hazardous Materials, **421**, 126673, **2022**.
34. LIU X., CHEN Z., WANG L., SHEN J. Effects of metal ions on THMs and HAAs formation during tannic acid chlorination. Chemical Engineering Journal, **211**, 179, **2012**.
35. DINÇ E., YAZAN Z., ERTEKIN Z., YILDIZ C. Two- and Three-Dimensional Strategies for Determining Consecutive Acidity Constants of Ciprofloxacin and Enrofloxacin Using Fluorescent Excitation-Emission Measurements. ChemistrySelect, **8** (27), e202301809, **2023**.
36. LI S., HUANG T., DU P., LIU W., HU J. Photocatalytic transformation fate and toxicity of ciprofloxacin related to dissociation species: Experimental and theoretical evidences. Water Research, **185**, 116286, **2020**.
37. SCISCENKO I., ARQUES A., VARGA Z., BOUCHONNET S., MONFORT O., BRIGANTE M., MAILHOT G. Significant role of iron on the fate and photodegradation of enrofloxacin. Chemosphere, **270**, 129791, **2021**.
38. WANG G., SHI W., MA D., GAO B. Impacts of permanganate/bisulfite pre-oxidation on DBP formation during the post chlorine disinfection of ciprofloxacin-contaminated waters. Science of the Total Environment, **731**, 138755, **2020**.